Taylor & Francis
Taylor & Francis Group

Vehicle System Dynamics
International Journal of Vehicle Mechanics and Mobility

ISSN: 0042-3114 (Print) 1744-5159 (Online) Journal homepage: https://www.tandfonline.com/loi/nvsd20

Noise, vibration, harshness model of a rotating tyre

Manfred Bäcker, Axel Gallrein & Michael Roller

To cite this article: Manfred Bäcker, Axel Gallrein & Michael Roller (2016) Noise, vibration, harshness model of a rotating tyre, Vehicle System Dynamics, 54:4, 474-491, DOI: 10.1080/00423114.2016.1158844

To link to this article: https://doi.org/10.1080/00423114.2016.1158844

VEHICLE SYSTEM DYNAMICS, 2016
VOL. 54, NO. 4, 474–491
http://dx.doi.org/10.1080/00423114.2016.1158844

IAVSD
Taylor & Francis
Taylor & Francis Group

Noise, vibration, harshness model of a rotating tyre

Manfred Bäcker, Axel Gallrein and Michael Roller

Fraunhofer ITWM, Abteilung MDF, Kaiserslautern, Germany

ABSTRACT

The tyre plays a fundamental role in the generation of acoustically perceptible driving noise and vibrations inside the vehicle. An essential part of these vibrations is induced by the road excitation and transferred via the tyre into the vehicle. There are two basic ways to study noise, vibration, harshness (NVH) behaviour: Simulations in time and frequency domains. Modelling the tyre transfer behaviour in frequency domain requires special attention to the rotation of the tyre. This paper shows the approach taken by the authors to include the transfer behaviour in the frequency range up to 250 Hz from geometric road excitations to resulting spindle forces in frequency domain. This paper validates the derived NVH tyre model by comparison with appropriate transient simulations of the base transient model.

ARTICLE HISTORY
Received 9 September 2015
Revised 22 February 2016
Accepted 23 February 2016

KEYWORDS
Tyre modelling; tyre simulation; vehicle simulation; NVH; rotating tyre; linearisation

1. Introduction

Drivers and passengers will perceive vibrations inside the vehicle as interference of their physical comfort. An essential part of these vibrations will be induced by the road excitation and be transferred via the tyre into the vehicle. The tyre itself acts as a resonator and therefore can damp or amplify the vibrations. One usually distinguishes between vibrations which lead to perceptible accelerations at the seat (comfort) and vibrations which increase the physical perceptible and audible noise levels inside the car. The vibrations in the comfort domain are covering the frequency range up to 150 Hz while the vibrations in the noise, vibration, harshness (NVH) domain are relevant up to 350 Hz, with these boundaries becoming increasingly blurred.

The tyre plays a fundamental role in the generation of acoustically perceptible driving noise and also in the generation of vibrations inside the vehicle. Depending on the type of assessment, the tyre can be seen either as a transmitter of the road excitations into the vehicle or as an integral part of vehicle subsystems (e.g. power train, braking system). In order to virtually emulate these mechanisms in the NVH context, different simulation techniques are being used by respectively different software tools.

There are in principle 2 different ways to study the NVH behaviour of a tyre or a full vehicle including tyre:

- Transient simulation scenario;
- Frequency-based or modal simulation scenario.

CONTACT Axel Gallrein axel.gallrein@itwm.fraunhofer.de

In the first case the tyre or the full vehicle will be simulated using a full transient dynamic simulation method. Doing this the driving manoeuvre could be arbitrary. The vehicle or the tyre is driving over an arbitrary digitised road profile. There is no need for a stationary driving state or for the necessity of a constant driving velocity. For the NVH assessment in this case typically one quantifies the acceleration level on the seat rail in time domain or in frequency domain. The advantage of the transient method is that one can simulate arbitrary events and driving manoeuvre and one can use a standard digitised geometric road profile. The disadvantage is that the simulation times and process turnaround times are relatively high which handicaps typical optimisation loops in product design.

In the second case one does a linearisation around a stationary state. With such a linear system one can do a typical modal analysis looking for Eigen frequencies (modal frequencies), corresponding mode-shapes, modal damping and so on. Moreover one can calculate the transfer-functions of the system which can be used to do a typical frequency response analysis which relates to a simulation of the linear system in frequency range. The advantage to simulate a linear system in frequency range is that such a simulation can be reduced to matrix multiplication and factorisations of the related transfer functions (transfer matrices) by the fft's of the system inputs. This leads to a very fast numerical scheme which is a big advantage compared to the fully transient approach. A disadvantage is that the linearisation of the system can be done only in a more or less stationary system state. Furthermore only small perturbation around this state could be observed. For the linearisation of a tyre an additional complications is the linearisation of the tyre/road contact. In the framework of a typical frequency response analysis the system inputs (and outputs) are time-series which will be transformed into frequency range using fft. This is possible without any problem if the tyre will be excited by a global contact patch excitation like on poster test rig. But if the preloaded tyre is rolling over a geometrically described 3D road one cannot easily transfer this situation into the standard context of a frequency response analysis.

As a summary one could state that both, the transient simulation approach and the frequency-based modal approach have their advantages and a right to exist. For both approaches the basis is an accurate dynamic model. The authors have developed a structural tyre model [1] that is used in the vehicle industry for transient simulations in comfort, durability and advanced handling scenarios. For purposes of validating the approach taken in frequency domain calculation, this model is used here in both approaches. After a very brief review of the model, the mechanical interface to the vehicle and the road is explained shortly.

In the second part of this paper, the linearisation around a rotating steady state is explained. Together with the mechanical interface, the linearisation gives rise to a linear state space equation that can then be used to construct the transfer behaviour of road excitation to spindle forces. The resulting transfer functions are validated against transient simulations with the same structural model and a transfer to frequency domain. These validations include both global contact patch excitations (poster scenarios) as well as local road excitations (rough road).

2. Structural model and mechanical interface

The authors have developed a structural multi body dynamic (MBD) tyre model [1] used in the vehicle industry for comfort, durability and advanced handling scenarios. This model

is based on a spatial finite difference (FD) formulation of the tyre modelled as a shell. The functional layers of a tyre (like cap ply, belt plies and carcass/body plies) are accumulated into the shell properties during tyre initialisation, but are accessible through their respective material parameters in the parameter file. The modelling of each cord-reinforced layer includes a nonlinear part in the elastic component of the material description due to different behaviour under compression and tension regimes. The geometric formulation of the material behaviour allows for very large deformations. The dissipative parts of the material description combine viscous–elastic and inner friction behaviour. The tread is modelled by a brush-type contact formulation, allowing for local stick–slip effects. Figure 1 sketches the principle functional components of this structural MBD tyre model next to the picture of the assembled model during a cleat run.

The mechanical interface between a vehicle model and a tyre model in an MBD context is standardised in the standard tyre interface. This original interface only includes the kinematic rigid body state of the wheel carrier plus tyre rotation relative to the road frame. It has been enhanced to include also the kinematic rigid body state of both rim and ground relative to world by several MBS tyre models, including the model used in this paper. Access to both is mandatory for applications like poster test rigs. From a viewpoint of the tyre, it receives both these kinematical rigid body states and returns accumulated force and moment vectors acting on the wheel centre and ideal road contact point accordingly. For the purpose of this paper, only the accumulated force and moment acting on the wheel centre are investigated. The local road surface roughness is typically a road surface model and describes the road surface geometry relative to the kinematic rigid body state of the ground body. Figure 2 sketches this interface in principle.

The authors have also expanded this interface to attach the tyre to a flexible representation of the rim as part of the vehicle model (see [2,3]). However, for the frequency range in consideration, the effect of the flexible rim has been neglected here. While this is feasible for aluminium rims, eventually for steel rims or an even further extension of the frequency

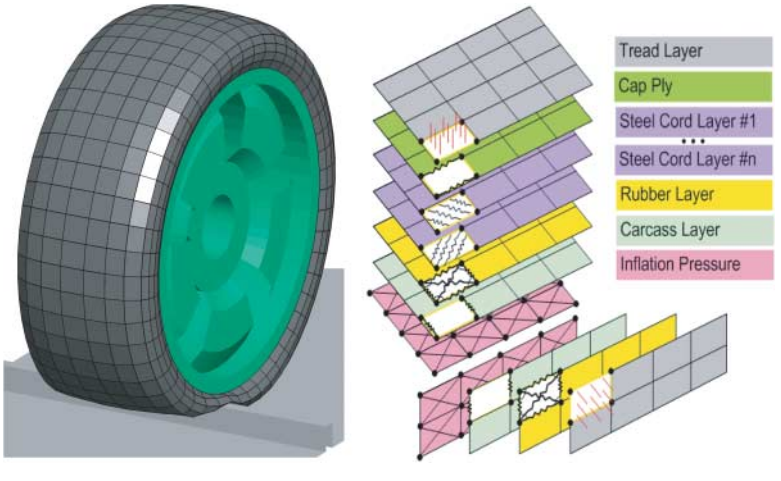

Figure 1. Left: picture of structural MBD tyre model running over a cleat. Right: principle functional layers included in shell-based formulation.

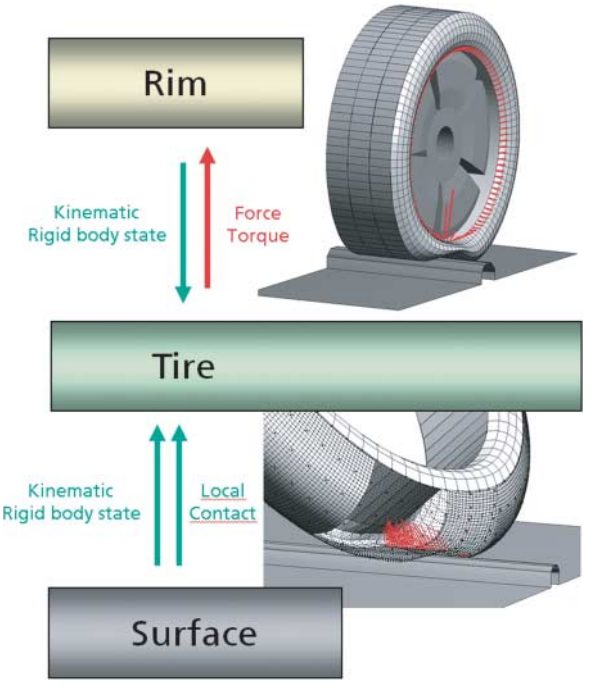

Figure 2. Principle sketch of the mechanical interface of an MBD tyre model.

range, this must be considered eventually. With the suggested interface from [2,3], this is in principle possible.

For the purpose of this paper, the mechanical interface from the viewpoint of the tyre can be summarised by:

- Inputs:
  - Rim kinematical rigid body state;
  - Ground kinematical rigid body state;
  - Local road surface heights in the contact area.
- Outputs:
  - Force and moment acting on wheel centre.

This interface scenario can in general be described by the following Equation (1), where u specifies the input displacements, $\dot{u}$ the input velocities, y specifies the outputs and x the internal degrees of freedom (both displacement and velocities):

$$\begin{aligned} M\dot{x} &= f(x, u, \dot{u}), \\ y &= g(x, u, \dot{u}). \end{aligned} \tag{1}$$

Note that the system (1) does not contain an explicit time dependence in both the rhs's of differential and output equation. It should also be noted that the differential equation part of (1) includes the reduction to first order of all second order differential

equations, with M being a block diagonal matrix consisting of the identity and the mass matrix.

3. Linearisation around steady state rolling

After having setup the overall dynamic model, this model has to be linearised. The linearisation will be done for a stationary rolling tyre. The overall state is defined by a specification of the following arbitrary but constant values:

- Preload;
- Velocity;
- Inclination angle;
- Toe angle.

For the linearisation, a method similar to the so called ALE (Arbitrary Lagrangian Eulerian) method has been used (see also [4,5] for a discussion on such methods). In this method, the stationary rolling tyre is described in a special spatial description instead of a material description. An important result in this method is the rise of gyroscopic forces acting on the tyre explicitly in the equation of motion (1). This is needed to introduce the correct velocity dependent modal behaviour into the linear system.

The tyre is now driven with a stand-alone tool to reach a steady state with the prescribed values of preload, velocity, inclination and toe angle. Once this is achieved, a special linearisation routine is executed. This routine performs the coordinate transformation to the previously mentioned Eulerian description and makes the resulting gyroscopic forces available. Once this is done, an FD scheme is executed to calculate the Jacobians of the rhs parts of Equation (1). As a result, the linear state space system is now available as ABCD matrices, as shown in Equation (2):

$$\begin{aligned} \dot{x} &= Ax + Bu + B'\dot{u}, \\ y &= Cx + Du + D'\dot{u}. \end{aligned} \tag{2}$$

For the purposes of this paper, the rotational degree of freedoms of the rigid rim around the axis of rotation for small rotations has been added to the system (2). As such, the moment around the rotational axis in y is zero. Also note that the matrix M from Equation (1) is a diagonal matrix for this system and the inversion with M needed to derive Equation (2) can be carried out easily.

4. Modal analysis of the rotating tyre

Matrix A from Equation (2) can be used in modal analysis. The additional gyroscopic forces introduce additional symmetric (centrifugal) and skew-symmetric (coriolis) layers in the A matrix. Without quantitative comparisons, some plausibility considerations can already be made at this point.

Figure 3 shows the frequency increase from 35 to 42 Hz for the Fore-Aft mode of the standing tyre vs. the rolling tyre at 30 m/s, both for 2.5 bar and 4000 N preload. The Fore-Aft mode is prominent in the longitudinal force of the rotationally free, but otherwise

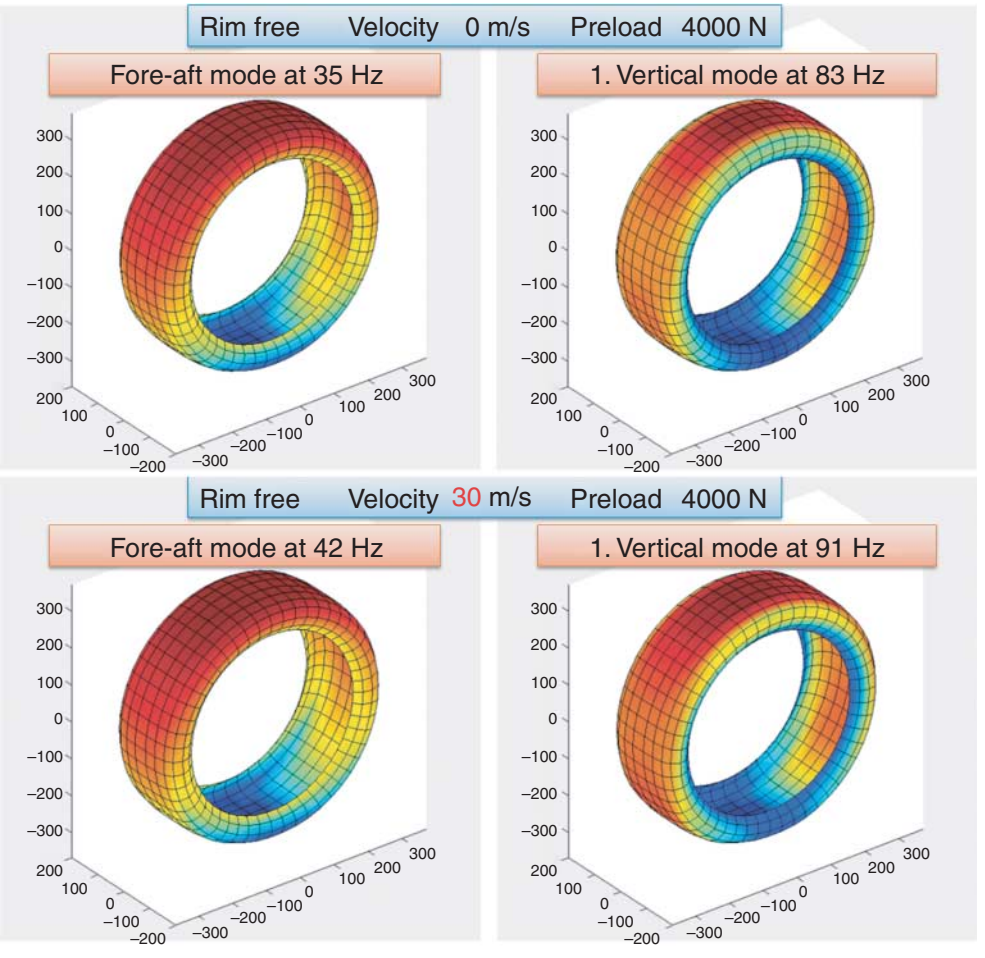

Figure 3. Frequency increase in Fore-Aft and first vertical modes of rotationally free rolling tyre at 4000 N preload from 0 to 30 m/s translational velocity.

constraint rim movement on flat surface, where the rim rotation is in-phase with the tyre rotation (and longitudinal translation). Figure 3 also shows the frequency increase from 83 to 91 Hz in the 1st vertical mode under the same variation. The first vertical mode is prominent in the vertical force of the rotationally free, but otherwise constraint rim on flat surface where the tyre translates in vertical direction. The frequency increase is due to the symmetric part in A from Equation (2), arising from the centrifugal forces in the additional gyroscopic forces.

Another plausibility consideration has been published by many authors (see [4–6]), and that is a frequency split of the same mode (in non-rotating conditions) to a mode shape that 'rotates' clock and counter-clockwise at different frequencies for the rotating tyre. Figure 4 shows the radial R3 mode for the inflated, non-deflected tyre rotating at an angular velocity of 100 rad/s to split in frequency of 114 Hz clockwise and 173 Hz counter-clockwise. As discussed in [4], this frequency split is due to the skew-symmetric parts (Coriolis) of the added gyroscopic forces due to the (unsymmetrical) transport velocity in the Eulerian description.

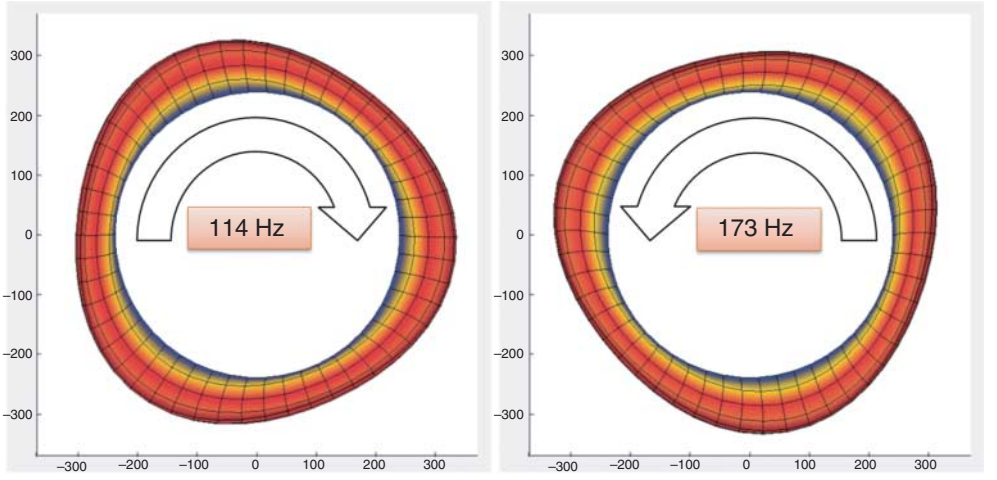

Figure 4. Frequency split of the same R3 mode for the inflated, free hanging tyre spinning with angular velocity of 100 rad/s.

5. Transfer behaviour of the rotating tyre

In order to validate some of the above presented plausibility considerations, the transfer behaviour of the transient, nonlinear model has been studied. For this purpose (and as an example), the transfer function (amplitude) of a vertical global contact patch excitation (poster scenario) to the longitudinal and vertical spindle force is shown in Figure 5 for the standing tyre and 4 velocities (10, 20, 30 and 40 m/s), all at 2.5 bar inflation pressure (solid lines) or 2.8 bar (dotted lines) and 4000 N preload. The transfer functions were calculated with a pink noise excitation with a range of ±1 mm for a duration of 100 s with a sampling rate of 10 kHz. The algorithm used was Matlab's tfestimate function (Hamming window with default length, 2048 overlap and 4096 blocklength).

Obviously, the transfer for the standing tyre of a global vertical road excitation to longitudinal spindle force is zero, as the tyre is rotationally symmetrical (a prerequisite for the method described to generate the transfer function in frequency domain). The increase in frequency of the Fore-aft mode from 35 Hz to well over 40 Hz can already be validated here. It is even more apparent in the Out-of-phase fore-aft mode at around 100 Hz. Interestingly, even for a velocity of 40 m/s, the out-of-phase fore-aft mode is excited in this scenario. This can be explained by the global vertical contact patch excitation, whereas it is known to be difficult to excite this mode with cleat runs, as standard cleats are too short wavelengthed to actually excite this mode for higher velocities. The increase in inflation pressure from 2.5 to 2.8 bar yields both an increase in frequency as well as amplitude for all major resonances. The inflation pressure variation was performed to show that the effect of velocity cannot be easily adapted by inflation pressure modification (as one example of parameter variation) – at least not within reasonable ranges. Interestingly, the amount of increase seems to depend nonlinearly on velocity.

Figure 5 also shows the corresponding vertical spindle force transfer. The increase in frequency of the 1st vertical mode from 83 to 93 Hz for 30 m/s and almost 100 Hz for 40 m/s translational velocity. As such, Figure 5 already validates the consistency of the *A*

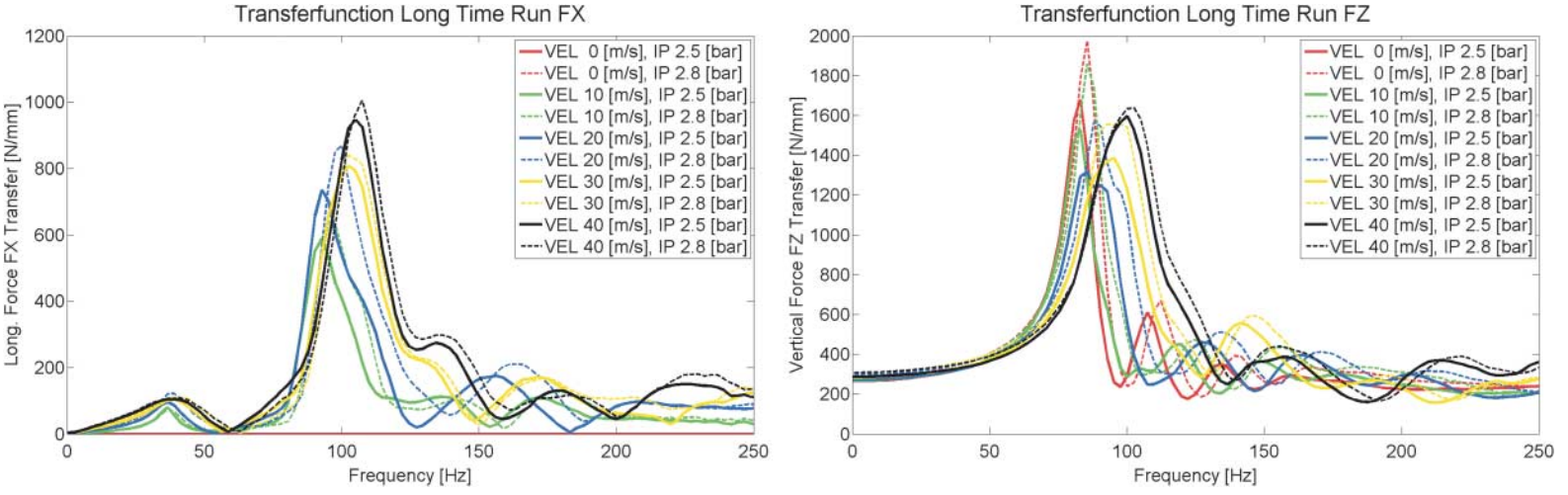

Figure 5. Transfer of global vertical road excitation to longitudinal (left) and vertical (right) spindle force.

matrix in Equation (2) – including the additional gyroscopic forces. Here, the inflation pressure variation also yields both an increase in frequency as well as amplitude for all major resonances. It may be worth mentioning that while the inflation pressure variation yields similar effects in both longitudinal and vertical spindle force transfer, the velocity variation does not. Whether this is due to the limited range of inflation pressure variation investigated here needs to be confirmed.

Laplace transformation of Equation (2) now yields the transfer function G, which can be evaluated at arbitrary frequencies $s = i2\pi f$:

$$\begin{aligned} y(s) &= G(s)\, u(s), \\ G(s) &= C(sI - A)^{-1}(B + sB') + D + sD'. \end{aligned} \tag{3}$$

This transfer behaviour can now be validated against the original, transient dynamic model. Figure 6 shows the same vertical transfer behaviour (from Figure 5) for the standing tyre against the calculated transfer behaviour of the linearised system (3).

Figure 7 now shows the transfer behaviour at 20 m/s (72 km/h) of both transient nonlinear model and transfer function calculated from the linearised model (3).

For any non-zero velocity, Figure 5 shows that there is also a transfer of the global vertical road excitation to the longitudinal spindle force. Figure 7 also compares this transfer behaviour against the transfer function calculated from the linearised model (3). Location of peaks in the 0.250 Hz range align perfectly between the estimated transfer behaviour of the transient simulation of the nonlinear model and the directly calculated transfer functions of the linearised model.

There is a small deviation between transient nonlinear and linearised model with respect to peak amplitude for the 3 resonances at 40 Hz and 95 Hz (FX) and 90 Hz (FZ). These peaks are less prominent in the nonlinear transient model but show a broader base. This is still under investigation, but currently believed to be due to frictional effects in the nonlinear model that cannot be linearised adequately. It should also be noted that the longitudinal force response (and the respective longitudinal transfer) is a consequence of the vertical

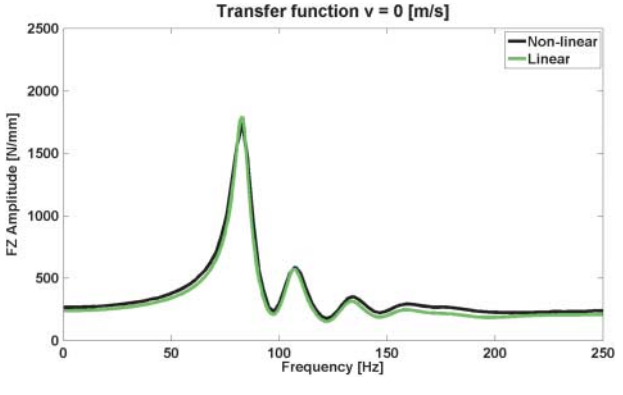

Figure 6. Transfer behaviour of global vertical road excitation to vertical spindle force – standing tyre at 2.5 bar and 4000 N preload.

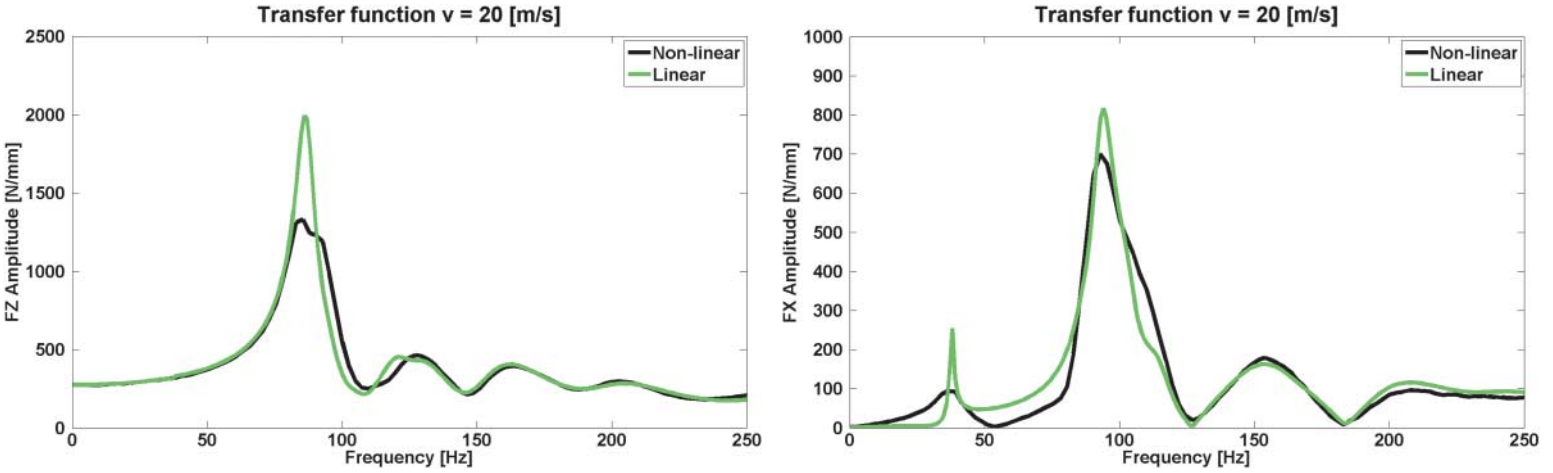

Figure 7. Transfer behaviour of global vertical road excitation to vertical spindle force – rolling tyre at 20 m/s (72 km/h) and 2.5 bar and 4000 N preload.

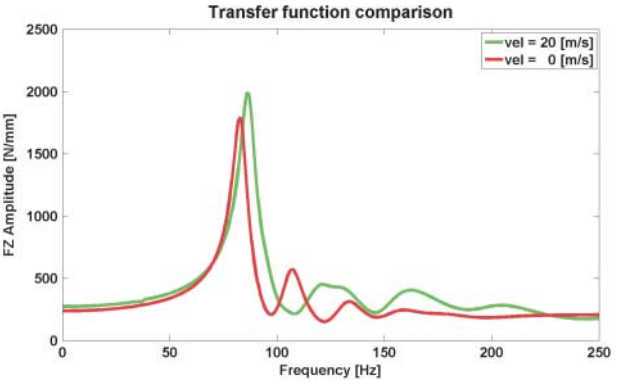

Figure 8. Transfer behaviour of global vertical road excitation to vertical spindle force – velocity dependence of linearised model.

global road excitation – there is no direct longitudinal road input. Rather, the longitudinal force is a consequence of the changes in the deflected radius due to the vertical road excitation for the vertically fixed spindle – and as such a pure dynamical effect, correctly predicted by the linearised model as well.

The main validation of these investigations is shown in Figure 8: The correct and validated velocity dependence of the linearised tyre on the transfer behaviour (taken from Figures 6 and 7), showing a significant velocity dependence already between 0 and 20 m/s (72 km/h):

Figure 8 also closes the analysis loop to the modal analysis results: The 1st vertical mode shift from 83 to 90 Hz is clearly visible.

As a final comparison for the global road excitation, the linear system (2) – including rim rotation – has been solved in time domain with the same pink noise excitation with a range of +/−1 mm, but limited to 5 s duration. Figure 9 now compares the calculated spindle response from these transient simulations of both nonlinear and linear model for the longitudinal spindle force at 20 m/s (72 km/h) for 2.5 bar and 4000 N preload.

For Figure 9 the more commonly used logarithmic scaling for the y axis has been used to show the response behaviour.

One challenging part in this linearisation process remaining is the condensation of the local road excitation. Formally, each point on the tyre surface in contact with the road surface for the linearised state of the tyre can have an independent excitation. However, some aspects have to be taken into account. The road excitation of contact points are not independent in the sense of mechanical excitation: the road surface 'travels' through the contact area, contact points on the same line of travel will experience the same road excitation, but with a time delay. In frequency domain, this time delay can be modelled as a phase shift for the respective contact point.

6. Local road excitation

To be able to simulate the linearised tyre rolling over a road surface with an arbitrary roughness (see Figure 10 for an example), it is necessary to set up a dedicated scenario to excite the contact patch of the tyre with local dynamic input(s).

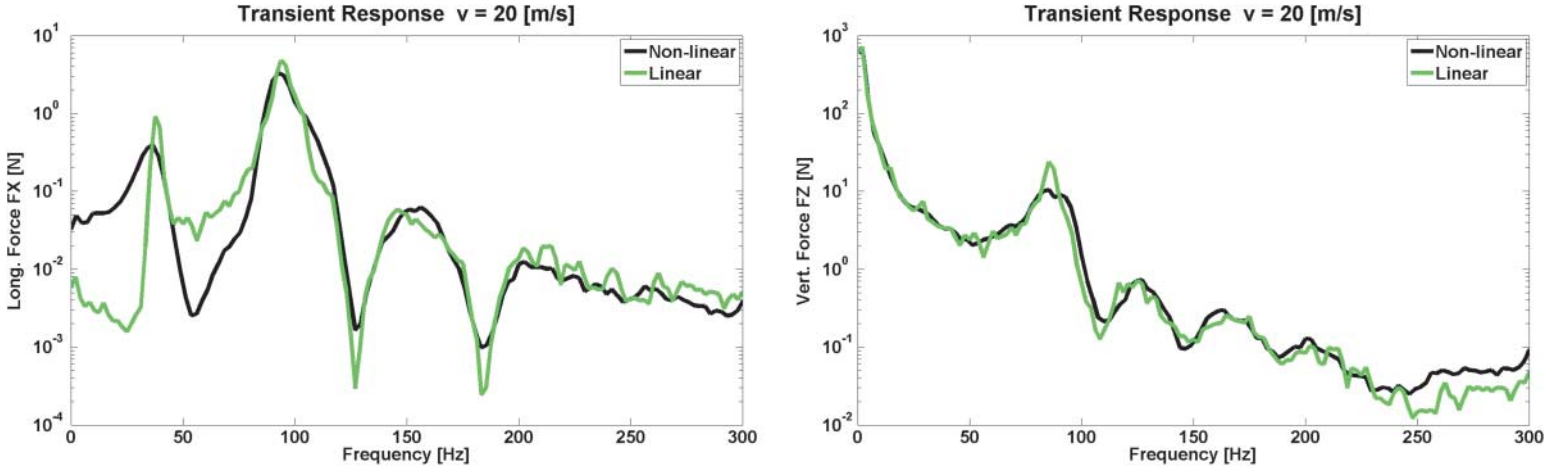

Figure 9. Transient response of longitudinal (left) and vertical (right) spindle force due to global vertical road excitation – Rolling tyre at 20 m/s (72 km/h) and 2.5 bar and 4000 N preload.

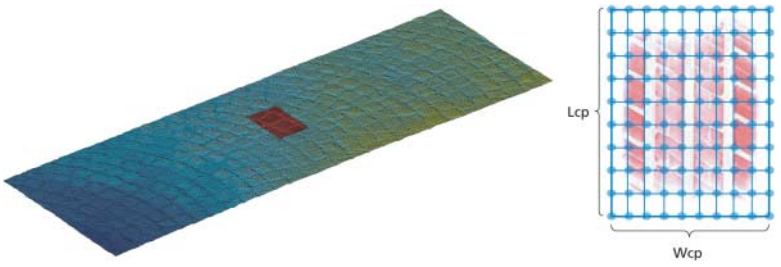

Figure 10. Small piece of a typical rough road (left) and road discretisation under tyre contact patch (right).

The linearised tyre is not able to roll any more – although the linearisation has been done for a rolling tyre with given velocity –because the linearisation is done in spatial coordinates (similar to the well-known ALE approach).

Therefore the road excitation has to be realised by an (local) time-dependent z-excitation of the tyre contact patch. In order to do this, we cover the contact patch by a rectangle of length Lcp and width Wcp. On this rectangle, a discrete, equidistant mesh of $Nx * Ny$ excitation nodes is defined. Nx and Ny can be chosen arbitrarily.

For each of these discrete road nodes, a time-dependent excitation can now be defined. To simulate the rolling of a tyre with a constant velocity v, the excitation signals lying in one line in x direction ($y = \text{const.}$) cannot be independent. For a tyre rolling with constant velocity v, two neighbour nodes in a line (same y coordinate) should have same excitation signal, but with a time delay of

$$\mathrm{d}t = v * \mathrm{d}x,$$
$$\mathrm{d}x = \frac{Lcp}{Nx - 1}.$$

Let $ZR_{j,k}\ (t)$ be the time-dependent z-excitation of the Node with index pair (j,k), where j describes the x-dimension and k the y-dimension of the road patch. Then the relation

$$ZR_{j+1,k}(t) = ZR_{j,k}(t - \mathrm{d}t)$$

has to be fulfilled to mimic a rolling of the tyre into positive x direction. By doing this, one can propagate a road unevenness through the tyre contact patch, which mimics the rolling over this unevenness.

If the road is given as a geometrical described road-profile in the spatial coordinates x, y and $z = \text{road}\ (x, y)$ and we are assuming – without loss of generality – that the tyre is rolling in positive x-direction, one can set

$$ZR_{j=1,k}(t) = \text{road}(v * t, y_0 + k \cdot \mathrm{d}y),$$
$$\text{where } \mathrm{d}y = \frac{Wcp}{Ny - 1},$$
$$ZR_{j+1,k}(t) = ZR_{j,k}(t = \mathrm{d}t) \text{ for } j = 2, \ldots, Nx.$$

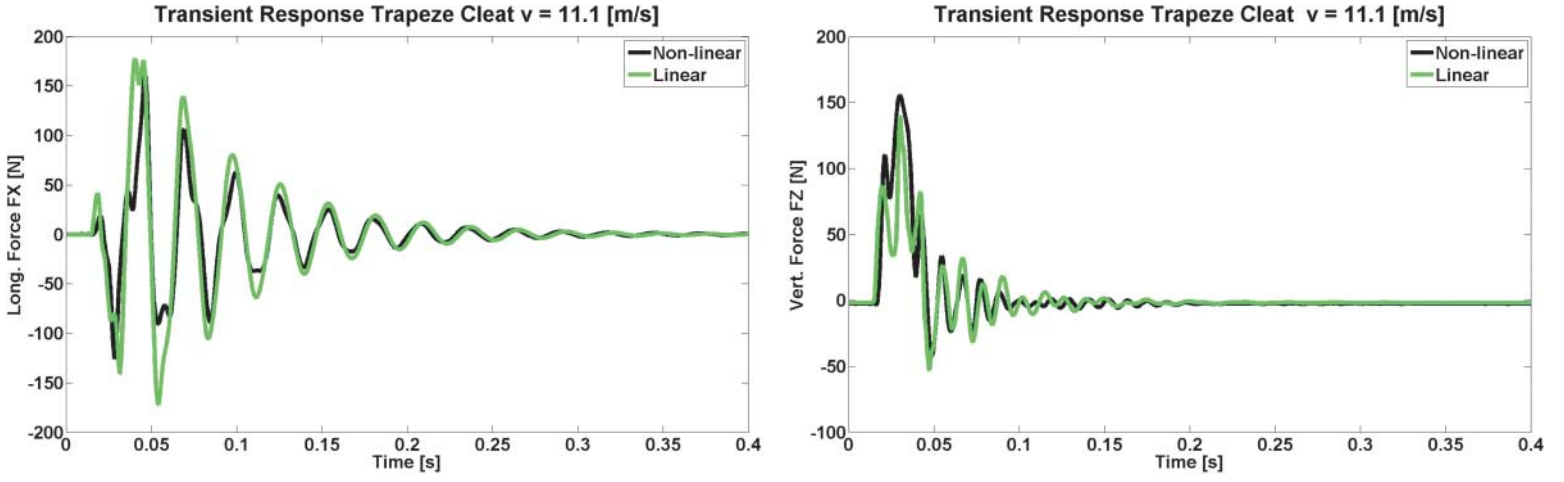

Figure 11. Transient response of longitudinal (left) and vertical (right) spindle force due to local vertical road excitation – at 10 m/s (36 km/h) and 2.5 bar and 4000 N preload rolling over an 4 × 200 mm cleat.

In frequency domain, this time delay yields a phase shift:

$$\mathcal{F}(ZR_{j+1,k})(\omega) = \mathrm{e}^{\mathrm{i}\omega\,\mathrm{d}t}\,\mathcal{F}(ZR_{j,k})(\omega)$$

with $\mathrm{d}t = v * \frac{Lcp}{Nx-1}$.

With this methodology, it is now possible to apply local road excitations to the linear system, both in the transient (time) and in the frequency domain. As an example, Figure 11 shows the transient response in longitudinal and vertical spindle force of the nonlinear model while running over a trapeze cleat of 4 mm height and 200 mm length, for 2.5 bar, 4000 N preload and a velocity of 10 m/s (36 km/h) and compares it to the linear model.

A cleat height of 4 mm is already a scenario that goes well into the nonlinear application range. This is reflected in the somewhat poor reproduction of the spindle forces (in both longitudinal and vertical direction) of the linear model – especially while driving of off the cleat ($t \sim 0.025$ s). While there are several nonlinearities to be taken into account, this example has been chosen as it features a prominent nonlinearity in the road excitation. The next chapter is dedicated on how to improve this scenario.

7. Golden tyre enveloping of road excitation

The somewhat unsatisfactory results shown in Figure 11 are mainly due to the mismatch of linear behaviour and reality. In the linear model, the road excitation is featured locally at contact points that are in contact on flat surface. A cleat however, especially a higher cleat, will impact the tyre geometrically sooner than at the point of first contact on flat surface – and leave the tyre later. This difference can be seen best in Figure 11, where the 'on-cleat' vertical force has a shorter duration for the linear model as the nonlinear model. It is even more dramatic in the other direction: a narrow but deep crack will almost not be seen at all by the nonlinear tyre, whereas a linear tyre will react even on the depth of such a crack.

To remedy this mismatch, the authors have implemented an approach that pre-processes the geometrical input data before they are applied to the linear model. In this approach, the road is scanned by a transient tyre run, outputting only the contact points that are in fact in

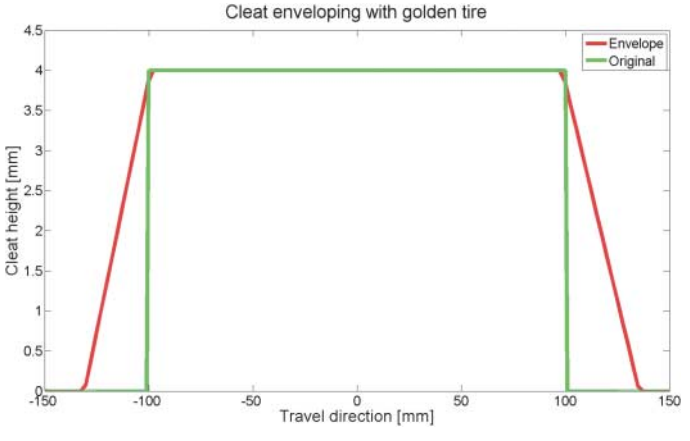

Figure 12. Enveloping of 4×200 mm cleat with golden tyre.

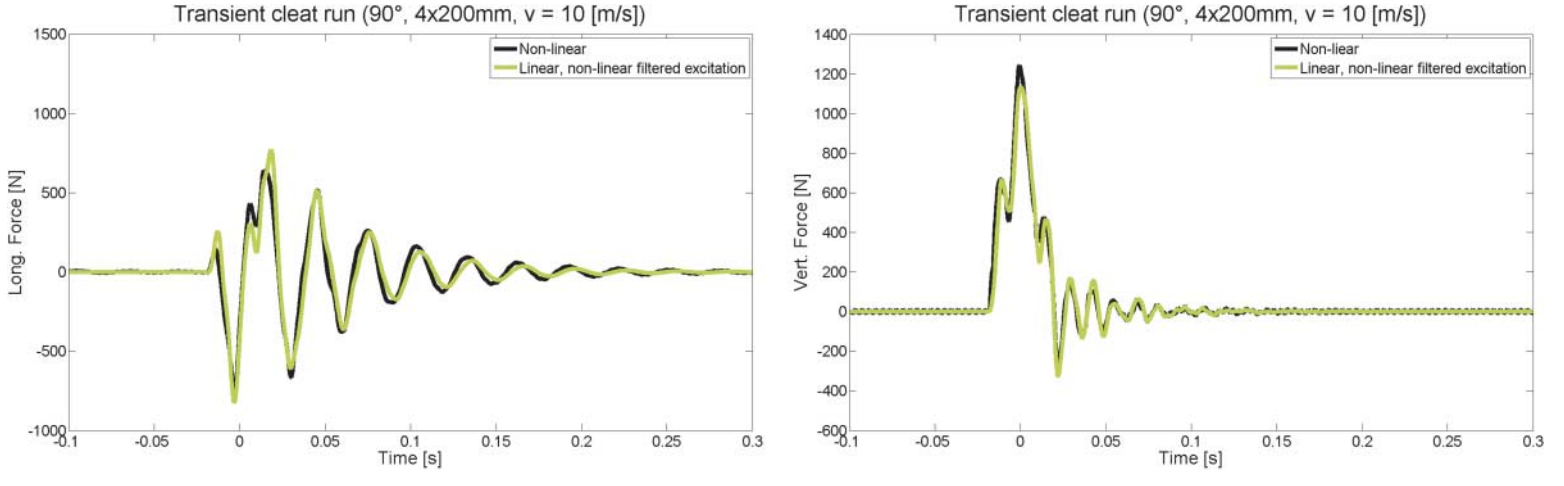

Figure 13. Transient response of longitudinal (left) and vertical (right) spindle force due to enveloped road excitation – at 10 m/s (36 km/h) and 2.5 bar and 4000 N preload rolling over an 4 × 200 mm cleat.

contact. It is important to note that the tyre used in this process does not need to reflect the properties of the original tyre very closely. The authors dubbed this tyre the 'golden tire'. In this example, the golden tyre used to envelope the road surface was a much wider tyre with significantly smaller aspect ratio. The envelope of the golden tyre for the 4×200 mm cleat is shown in Figure 12.

When the enveloped data is used as input in the linear model, the resulting spindle forces are much more accurate. Figure 13 shows the same comparison as Figure 11– but with enveloped data as input for the linear model.

8. Summary/conclusions

The authors have described a method to transfer their structural tyre model – in many cases successfully used in transient simulation scenarios – into a frequency-based simulation scenario very often used for NVH analysis because of low CPU consumption.

The implementation of this method has been realised by setting up a tool to linearise a rolling tyre around an arbitrary state (preload, velocity, camber, toe angle). To overcome the fact that a rolling tyre is not in a static equilibrium, the residual gyroscopic forces have been included in the linearisation scheme. By doing this in a proper way, the authors could show that the expected mode-split due to the velocity could be observed for rotating hanging tyre and for the rotating deflected tyre.

A second problem to overcome in the linearisation is utilisation of the road excitation because the linearisation is done in spatial coordinates like in the well-known ALE approach and therefore the linear tyre model does not rotate any longer. While it is quite straight forward to realise a global contact patch excitation (e.g. in a poster scenario), a local contact patch excitation is a challenge. The authors described a method which solves this problem by setting up a special road surface model.

With the overall linearised system of the rotating tyre one can then do a simulation in time domain and one can additionally directly derive a transfer function in frequency domain from this system. Both approaches have been validated. For the validation, the authors used references created by respective simulations using the nonlinear tyre model in time domain. In a first step, the linearisation could be successfully verified for the global excitation scenario by comparing on transfer function level and on response level in frequency domain. In a second step the local road excitation scenario could be successfully verified for a single cleat event. For larger cleats, a special process of enveloping the road excitation with a golden tyre has to be applied to the input data before application in the linear system to reach the desired accuracy.

Currently the authors are in preparation to setting up suitable interface to NVH-tools to import the linearised tyre model in these tools to utilise the usage in full vehicle simulation scenarios. After having this available, the full vehicle NVH analysis can be done extremely performant in frequency domain simulations. Moreover, a modal analysis of the overall vehicle including the rolling tyre could be performed by importing the system matrices adequately into the vehicle model.

Disclosure statement

No potential conflict of interest was reported by the authors.

References

[1] Gallrein A, Baecker M, Gizatullin A. Structural MBD tire models: closing the gap to structural analysis – history and future of parameter identification. SAE Technical Paper 2013-01-0630, 2013, doi:10.4271/2013-01-0630.

[2] Baecker M, Gallrein A, Heim R. Exploring new fields of virtual load prediction by accurate tire simulation for large deformations and flexible rim support. Mater.wiss Werkst.tech. 2011;42(10):909–920.

[3] Baecker M, Gallrein A, Hack M, Toso A. A method to combine a tire model with a flexible rim model in a hybrid MBS/FEM simulation setup. SAE Int. SP-2307, 2011-01-0186; 2011.

[4] Brinkmeier M, Nackenhorst U. An approach for large-scale gyroscopic eigenvalue problems with application to high-frequency response of rolling tires. Comput Mech. 2008;41/4:503–515. doi:10.1007/s00466-007-0206-6

[5] Lopez I, Blom R, Roozen N, Nijmeijer H. Modelling vibrations on deformed rolling tires – a modal approach. J Sound Vib. 2007;307(3–5):481–494. doi:10.1016/j.jsv.2007.05.056

[6] Baecker M, Gallrein A, Roller M. From road excitation to spindle forces in frequency domain: linearization of the rolling tire. SAE Technical Paper 2015-01-0625; 2015. doi:10.4271/2015-01-0625.